

Thermal Fluctuations Limit the Adhesive Strength of Compliant Solids

Tian Tang

Anand Jagota

Manoj K. Chaudhury

Department of Chemical Engineering, Lehigh University, Bethlehem, Pennsylvania, USA

Chung-Yuen Hui

Department of Theoretical and Applied Mechanics, Cornell University, Ithaca, New York, USA

For compliant solids, the stress required to separate an interface (its adhesive strength) appears to be much lower than that calculated by computing intersurface interactions. We explore the hypothesis that the adhesive strength is limited in value by thermal fluctuations. In a simple model of an interface, molecules bridging the two surfaces are represented by linear entropic springs. Asymptotic and numerical analyses are carried out to evaluate the adhesive strength and effective work of adhesion. For stiff materials, adhesive strength is found to be equal to the intrinsic strength—the maximum value of intersurface stress computed ignoring fluctuations. For compliant materials, adhesive strength is significantly reduced and is on the order of the elastic modulus. The effective work of adhesion agrees with the intrinsic work of adhesion for stiff materials and can decay slowly with increasing compliance.

Keywords: Adhesive strength; Compliance; Statistical model; Thermal fluctuation; Work of adhesion

1. INTRODUCTION

Two physical quantities are usually used to characterize the adhesion between solids: the stress needed to separate the interface and the

Received 12 November 2005; in final form 17 March 2006.

One of Collection of papers honoring Hugh R. Brown, who received *The Adhesion Society Award for Excellence in Adhesion Science, Sponsored by 3M*, in February 2006.

Address correspondence to Anand Jagota, Lehigh University, Department of Chemical Engineering, 111 Research Drive, Bethlehem, PA 18015, USA. E-mail: anj6@lehigh.edu

work absorbed in the separation process. For elastic solids with no bulk energy dissipation, the primary resistance to crack growth on the interface is provided by intermolecular forces, *e.g.*, van der Waals interactions in the case of unbonded interfaces. Based on molecular theories [1], a typical plot of the applied stress *versus* displacement has an increasing branch at relatively small displacement and a decreasing branch at relatively large displacement. The stress at which the two branches meet is the upper limit for the applied stress and is referred to as the intrinsic adhesive strength, σ_o . The area under the stress-displacement curve is the energy to fracture a unit area of the interface and is the intrinsic work of adhesion, W_{ad} . These two quantities are connected through the cohesive zone theory of fracture, first proposed by Dugdale [2] and Barenblatt [3].

The adhesive strength, σ_o , is on the order of W_{ad}/δ_o , where δ_o is a characteristic length representing the separation between the two surfaces. If one imagines that the bodies are separated as rigid entities, the characteristic length, δ_o , derives from the inter-surface potential and is of order nanometers to angstroms. For van der Waals types of interactions, W_{ad} is about 50–100 mJ/m². Using these numbers, the intrinsic adhesive strength, σ_o , is found to be 10^2 – 10^3 MPa. For stiff materials, defined here as those with elastic modulus much greater than intrinsic strength, such a value poses no problem. However, for compliant materials such as gels and elastomers, the intrinsic strength can be much larger than the elastic modulus. How can a material separation process require the imposition of surface tractions so much in excess of its elastic modulus? Indeed, it has been shown by Hui *et al.* [4] that if σ_o is much larger than the elastic modulus, E_M , a crack tip in the material tends to blunt instead of propagating. Therefore, the failure of the interface must often occur by some process that can operate at a stress on order of or lower than the elastic modulus. An example of such a process is elastic cavitation [5]; other possibilities are discussed in Ref. [4]. Nevertheless, interfacial separation does eventually occur.

To our knowledge, there are no conclusive and direct measurements of the adhesive strength. However, its value is an important determinant of the relationship between intrinsic work of fracture and dissipative mechanisms, *e.g.*, viscoelastic or plastic deformation [6,7], and, thus, can be inferred. The adhesive strength to match the experimental data of Mazur and Plazek [8] on the coalescence of acrylic beads was found by Lin *et al.* [9] to be on the order of 1 MPa, two orders of magnitude smaller than σ_o predicted by van der Waals interactions. The adhesive stress used by Jagota *et al.* [10] to match experiments on decohesion of a viscoelastic polymer was again on the order of the modulus. The critical stress at which cavitation occurs at the interfaces of cross

linked rubbers and hydrophobic solids also is a fraction of 1 MPa, [11,12]. Another interesting example is the Johnson-Kendall-Roberts (JKR) test [13]. This test has been used to measure the surface energy of soft polymers [14]. The modulus of these polymers is on the order of 1 MPa, which is at least two orders of magnitude lower than the intrinsic strength of the interface. This means that the stress at the edge of the contact zone must exceed the elastic modulus of the polymer by two orders of magnitude! This result is difficult to reconcile by a stress concentration argument, especially in light of the fact that the air gap just outside the contact zone is typically very sharp, which is consistent with small deformation. Thus, one is led to the inescapable conclusion that the adhesive stress of soft solids is much lower than its intrinsic value. On the other hand, despite this inconsistency with van der Waals theory concerning adhesive strength, the work of adhesion in a JKR test is in good agreement with the van der Waals theory—a paradox!

These considerations raise the following questions. In compliant materials, why is the stress required to separate the interface so much lower than its value computed by integrating intermolecular forces between the two bodies? That is, how can the interface fail under a load that is much smaller than the load needed to conquer the intermolecular attraction?

A calculation of intersurface forces between two bodies implicitly assumes that the molecules in the two solids are frozen at their location. That is, although fluctuations of thermal photons are included at a fundamental level in the Lifshitz theory used to calculate van der Waals forces, molecules themselves are not allowed to fluctuate in space. This is the case of zero temperature or very low compliance. At higher temperature or higher compliance, however, one would expect thermal fluctuations of the molecules. Although this is generally true for all solids, in this article we will imagine the space between the two solids as being occupied by a layer of bridging chains, germane to polymeric solids. Each of these chains undergoes stretching and has a finite probability of detaching from one of the surfaces. The number of undetached chains follows thermodynamic statistics and decays rapidly with the applied displacement. Because the external stress is balanced by the tension in the chains, the actual adhesive stress can be lowered considerably by thermal fluctuations.

A statistical chain-breaking model has been used by Chaudhury *et al.* [14,15] in their study of rate-dependent fracture on polymeric interfaces. (See also Refs. [15] and [16] for references to other previous models of adhesion based on kinetics of detachment or breakage of molecules.) Hui *et al.* [17], using a similar approach, provided closed-form solutions for the fracture toughness of a growing crack at very

high or very low speed. However, these works did not address the question of interfacial strength.

In this work, we ask the following questions: Can thermal fluctuations allow an interface to separate without having to go over the van der Waals peak stress? More specifically, how does the adhesive strength depend on material properties and the intrinsic work of separating the interface? We consider only equilibrium situations here, but the framework can be extended to study rate-dependent interfacial separation.

The plan of the article is as follows. In Section 2, we explain how we model the interactions between two solids by introducing thermal fluctuations. Adhesive stress and effective work of adhesion are formulated using this model. In Section 3, we provide numerical results for adhesive stress and effective work of adhesion. Asymptotic analyses, carried out in Section 4, provide closed-form solutions in various limits that are in excellent agreement with numerical results. We conclude in Section 5 with a summary of our results.

2. MODEL

Consider two solids separated by a distance u , as drawn in Figure 1. For simplicity, let us assume thermal fluctuations on only one of the solids, solid 2 on the right. That is, the molecules of solid 2 are mobile. Their positions can vary and approach surface 1. The distance from the end of a molecule to surface 1 is denoted by δ . We assume

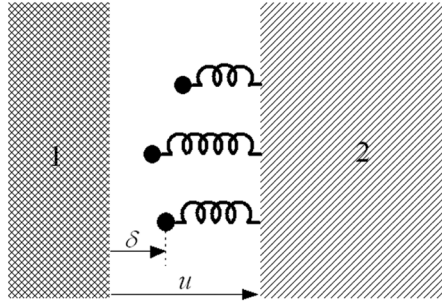


FIGURE 1 Surfaces of two solids at a distance u . Solid 1 is assumed to be rigid with a smooth surface, whereas molecules in solid 2 fluctuate thermally under the influence of van der Waals attraction from solid 1 and a restoring force linear in the extension of the molecule itself.

van der Waals interaction between the two solids. The van der Waals attraction tends to stretch molecules towards surface 1, while a restoring spring force tends to pull them back. Hence, there are two contributions to the total energy between the two solids. Two important parameters expected to govern the relationship between effective and intrinsic strength are temperature and compliance.

Modeling the bridging molecules as linear springs with compliance C [18], the energy associated with a particular molecule can be written as

$$E(u, \delta) = \frac{(u - \delta)^2}{2C} - \frac{W_{ad}}{\Sigma_o} \left(\frac{\delta_o}{\delta + \delta_o} \right)^2, \quad (1)$$

where Σ_o is the number of molecules per unit area on surface 2, W_{ad} is the intrinsic work of adhesion, and δ_o is a cutoff distance in the van der Waals interaction. The first term represents the energy in the stretched spring; the second term represents the van der Waals energy of attraction. (See Appendix A for details.) Figure 2 gives an example of $E(u, \delta)$ as a function of δ . Each term in Equation (1) is plotted separately. It can be seen from this figure that $E(u, \delta)$ generally contains two minima. One of them is at $\delta = 0$ (circle) and represents the bound state. The other is at $\delta \cong u$ (triangle) and represents the unbound state. In general, a molecule can pick from a continuum of states, but it has higher probability of staying near the energy minima. As is shown later, for small u , the second minimum at $\delta \cong u$ vanishes, and most of the molecules stay in the bound state at $\delta = 0$. As u increases, the

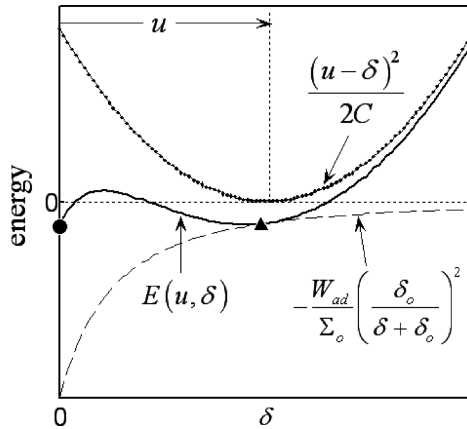


FIGURE 2 Energy $E(u, \delta)$ as a function of δ and each term in Equation (1). $E(u, \delta)$ shown in this figure has two minima, one at $\delta = 0$ (circle) and the other at $\delta \cong u$ (triangle).

second minimum appears, and the shallow energy well at $\delta \cong u$ allows more and more molecules to stay in the unbound state. Our goal in this work is to determine where the molecule will try to “sit” for a given u and to use that information to compute thermodynamic quantities.

Our simple model attempts to represent the fact that, especially for compliant molecules, many detached states are made available as the molecules are stretched. The conjecture is that well before the molecule is stretched so much that its attached state is at intrinsic adhesive strength, most chains will already be in the detached state. This mechanism will then limit the strength of the interface.

In equilibrium, at a given value of separation, u , molecules will have a variety of different extensions, δ . If we can calculate the probability density for a particular extension, we can then use this information to compute the mean force resisting the applied separation, which is what we desire to know. To do this, we formulate a partition function for our model. This can be used to derive all the physical quantities we need using Boltzmann statistics [19]. In particular, we treat W_{ad} in Equation (1) as fixed and determine how compliance, C , and temperature, T , affect the adhesive strength and effective work of fracture.

Given u , the partition function, $Z(u)$, under isothermal condition, is by definition the sum of the Boltzmann factor $e^{-E(u,\delta)/kT}$ over all possible states [19], where k is the Boltzmann constant and T is temperature. Because, for a given u , different states correspond to different δ , the partition function is given by

$$Z(u) = \frac{1}{\delta_o} \int_0^\infty e^{-E(u,\delta)/kT} d\delta, \quad (2)$$

where δ_o has been chosen to normalize the integral so that $Z(u)$ is dimensionless. As is well known, this normalization has no effect on thermodynamic properties. We allow δ to vary from 0 to ∞ , *i.e.*, the end of the molecule is *a priori* allowed to explore any position from contact with the rigid surface to infinite separation from it to the right. Actual positions of the molecule are always confined for $\delta > u$ by the quadratic spring potential and for $\delta < u$ either by the rigid surface (for small u) or again by the spring potential. A more realistic restoring potential for the spring will likely be asymmetric about u , not quadratic. In particular, we might expect a greater energetic penalty for $\delta > u$ than for $\delta < u$. We have explored a few different options for potentials that capture this physical feature. Results based on these more complicated potentials appear not to change qualitatively any of our conclusions but add considerable complexity. Therefore, for the sake of simplicity, we have adopted the simple potential given in Equation (1).

A number of physical quantities can be obtained from the partition function. For example, the Helmholtz free energy is related to Z by [19]

$$G(u) = -kT \ln Z, \tag{3}$$

and the average internal energy is

$$\langle E \rangle = \frac{\int_0^\infty E(u, \delta) e^{-E(u, \delta)/kT} d\delta}{\int_0^\infty e^{-E(u, \delta)/kT} d\delta} = -\frac{1}{Z} \frac{\partial Z}{\partial (1/kT)}, \tag{4}$$

The mean adhesive stress is

$$\sigma(u) = \Sigma_o \frac{\partial G(u)}{\partial u} = -\frac{\Sigma_o kT}{Z} \frac{\partial Z}{\partial u}. \tag{5}$$

Substituting Equations (1) and (2) into Equation (5) results in

$$\sigma(u) = \frac{\Sigma_o \int_0^\infty (u - \delta) e^{-E(u, \delta)/kT} d\delta}{C \int_0^\infty e^{-E(u, \delta)/kT} d\delta}. \tag{6}$$

This result is clearly identifiable as the average force on a chain times its areal number density. The effective work of adhesion is the change in Helmholtz free energy of the system with the two surfaces in contact and remote from each other:

$$W_{eff} = \Sigma_o \int_{u_o}^\infty \sigma(u) du = \Sigma_o [G(\infty) - G(u_o)], \tag{7}$$

where u_o is the displacement where the average stress is zero, *i.e.*, $\sigma(u_o) = 0$. Note that at zero stress the displacement is itself nonzero, in general; zero stress is at some small value of separation, u_o . However, numerical computations show that its value is small. More specifically, the work to separate the interface from $u = 0$ to u_o is negligible. Because in general u_o cannot be obtained explicitly, we make the following approximation:

$$W_{eff} \approx \Sigma_o [G(\infty) - G(0)], \tag{8}$$

i.e., we neglect the work required to separate the two surfaces from 0 to u_o . This approximation has been validated numerically.

To expedite the analysis, we introduce the following normalization:

$$\begin{aligned} u &\equiv \delta_o \bar{u}, & \delta &\equiv \delta_o \bar{\delta}, & E &\equiv kT \bar{E}, \\ G &\equiv kT \bar{G}, & \sigma &\equiv \frac{2W_{ad} \bar{\sigma}}{\delta_o}, & W_{eff} &\equiv W_{ad} \bar{W}_{eff}. \end{aligned} \tag{9}$$

Variables \bar{u} and $\bar{\delta}$ are, respectively, the normalized separation and end-to-surface distance. \bar{E} and \bar{G} are, respectively, the normalized internal energy and free energy. $\bar{\sigma}$ is the adhesive stress normalized by the peak van der Waals stress, *i.e.*, the intrinsic strength $2W_{ad}/\delta_o$, and \bar{W}_{eff} is the effective work of adhesion normalized by the intrinsic work of adhesion.

By using Equation (9), we can write Equations (1–4), (6), and (8) as

$$\bar{E}(\bar{u}, \bar{\delta}) = \frac{\Lambda(\bar{u}, \bar{\delta})}{\bar{T}}, \quad (10a)$$

$$Z(\bar{u}) = \int_0^\infty e^{-\Lambda(\bar{u}, \bar{\delta})/\bar{T}} d\bar{\delta}, \quad (10b)$$

$$\bar{G}(\bar{u}) = -\ln Z, \quad (10c)$$

$$\langle \bar{E} \rangle = -\frac{1}{Z\bar{T}} \frac{\partial Z}{\partial(1/\bar{T})}, \quad (10d)$$

$$\bar{\sigma}(\bar{u}) = \frac{3}{\bar{C}} \left[\bar{u} - \frac{I(\bar{u})}{Z(\bar{u})} \right], \quad (10e)$$

$$\bar{W}_{eff} \approx \bar{T}[\bar{G}(\infty) - \bar{G}(0)], \quad (10f)$$

where

$$\Lambda(\bar{u}, \bar{\delta}) \equiv \frac{3}{\bar{C}}(\bar{u} - \bar{\delta})^2 - \frac{1}{(1 + \bar{\delta})^2}, \quad \bar{T} \equiv \frac{\Sigma_o kT}{W_{ad}}, \quad \bar{C} \equiv \frac{6W_{ad}C}{\Sigma_o \delta_o^2}, \quad (11)$$

$$I(\bar{u}) \equiv \int_0^\infty \bar{\delta} e^{-\Lambda(\bar{u}, \bar{\delta})/\bar{T}} d\bar{\delta}. \quad (12)$$

In Equation (11), $\Lambda(\bar{u}, \bar{\delta})$ is the normalized energy function. For fixed W_{ad} , \bar{T} can be treated as a normalized temperature, and \bar{C} is a normalized compliance. $I(\bar{u})$ in Equation (12), when normalized by $Z(\bar{u})$, can be considered as the average position of the end of a generic chain at a given separation, u .

We first show that for the case of extremely low temperature, *i.e.*, $\bar{T} \rightarrow 0$, the effective work of adhesion, W_{eff} , approaches the intrinsic work of adhesion, W_{ad} . Specifically, according to Equations (10c) and (10f), to evaluate \bar{W}_{eff} , we need to evaluate the partition function in the unbound state where $\bar{u} \rightarrow \infty$ and in the bound state where $\bar{u} \rightarrow 0$. In the unbound state, as $\bar{u} \rightarrow \infty$, the normalized energy

$\Lambda(\bar{u}, \bar{\delta})$ defined in Equation (11) is essentially governed by the quadratic term $3(\bar{u} - \bar{\delta})^2/\bar{C}$. That is, a molecule fluctuates in the confining harmonic potential. The partition function can be approximated by

$$Z(\infty) \approx \lim_{\bar{u} \rightarrow \infty} \int_0^\infty e^{-(3/\bar{C}\bar{T})(\bar{u}-\bar{\delta})^2} d\bar{\delta} = \sqrt{\frac{\pi\bar{C}\bar{T}}{3}}. \quad (13)$$

In the bound state, as $\bar{u} \rightarrow 0$, $\Lambda(0, \bar{\delta}) = 3\bar{\delta}^2/\bar{C} - 1/(1 + \bar{\delta})^2$ is a monotonically increasing function of $\bar{\delta}$. The rapid decay of the exponential factor in the partition function implies that the value of the partition function is determined by the behavior of $\Lambda(0, \bar{\delta})$ near its global minimum, which occurs at $\bar{\delta} = 0$. Hence

$$Z(0) \approx \int_0^\infty e^{-(1+2\bar{\delta})/\bar{T}} d\bar{\delta} = \frac{\bar{T}e^{1/\bar{T}}}{2}. \quad (14)$$

Using Equations (10c,d), (13), and (14), it can be shown that as $T \rightarrow 0$, both $\bar{G}(\infty)$ and $\langle \bar{E}(\infty) \rangle$ go to zero, whereas both $\bar{G}(0)$ and $\langle \bar{E}(0) \rangle$ go to $-1/\bar{T}$. The latter is expected because the free energy and the mean internal energy should become the intrinsic adhesion energy when the two surfaces are in contact at 0 K. The normalized effective work of adhesion, \bar{W}_{eff} , according to Equation (10f), is therefore unity, that is, $W_{eff} = W_{ad}$.

3. NUMERICAL RESULTS

We now consider the more general case where \bar{T} is finite. For soft materials such as poly (dimethylsiloxane) (PDMS) with van der Waals type of interaction, the intrinsic work of adhesion is about $W_{ad} \approx 50 \text{ mJ/m}^2$ [15]. Take a typical value of areal number density $\Sigma_o \approx 1 \times 10^{18} \text{ m}^{-2}$. Using these numbers, \bar{T} at room temperature is about 0.08, which is much less than 1, and this is the limit we are most concerned with in this work.

The adhesive stress and effective work of adhesion is determined by Equations (10e) and (10f), respectively. Thus, the problem reduces to the evaluation of $Z(\bar{u})$ and $I(\bar{u})$. In the following, we present the results for the adhesive stress and effective work of adhesion evaluated by numerically integrating $Z(\bar{u})$ and $I(\bar{u})$. These numerical results are compared with asymptotic solutions, which are presented in the next section.

Figure 3 plots $\bar{\sigma}(\bar{u})$ versus \bar{u} for $\bar{T} = 0.08$ and different values of normalized compliance, \bar{C} . Symbols are numerical results, and solid lines are asymptotic solutions. Figure 3 shows that the adhesive stress

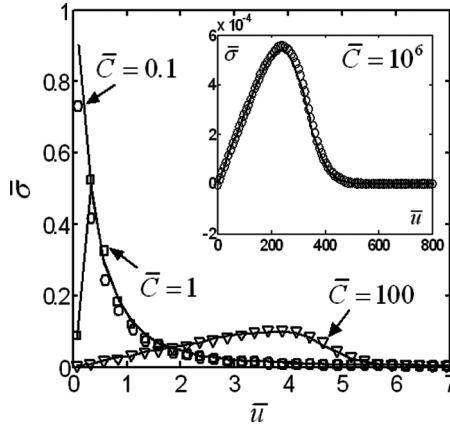


FIGURE 3 Normalized adhesive stress *versus* normalized separation. For each \bar{C} , symbols are results obtained by numerical integration of $Z(\bar{u})$ and $I(\bar{u})$, and the solid line represents an asymptotic solution given in Section 4.

increases linearly with separation for small \bar{u} . This represents the fact that almost all the springs are at the bound state and are being pulled out. Indeed, using Equation (10e) and our asymptotic solution (19a,b), one can easily show that, as long as $\bar{u} \ll \bar{C}/3$ and $\bar{C} \gg 3\bar{T}/2$,

$$\bar{\sigma} \cong \frac{3}{\bar{C}} \left(\bar{u} - \frac{\bar{T}}{2} \right), \tag{15a}$$

which, in dimensional form, is

$$\sigma \cong \frac{\Sigma_o}{C} \left(u - \frac{\Sigma_o kT}{2W_{ad}} \delta_o \right). \tag{15b}$$

The first term in Equation (15b) represents the restoring spring force. The negative term captures the fact that zero stress occurs at a slightly positive value because of entropic repulsion from the hard wall. The decay of the adhesive stress after its peak indicates that the number of springs in contact is falling off rapidly with increasing displacement.

Figure 3 shows that for small compliance ($\bar{C} \ll 1$), *i.e.*, for very stiff materials, the normalized peak stress approaches unity, indicating that σ_{max} approaches $2W_{ad}/\delta_o$, the intrinsic strength. The peak stress decreases considerably as the compliance increases. An estimate of \bar{C} for compliant materials (*e.g.*, PDMS), based on the entropy of freely jointed chains, is [18]

$$C = \frac{Nb^2}{3kT}, \tag{16}$$

where b is the Kuhn length, and N is the number of rigid segments in one chain, *i.e.*, the total length of the chain divided by b . Taking $b = 2 \text{ nm}$ and $N = 1000$, C at room temperature is about 10^5 m/N . Using $W_{ad} = 50 \text{ mJ/m}^2$, $\Sigma_o = 1 \times 10^{18} \text{ m}^{-2}$ and $\delta_o = 1 \text{ \AA}$, \bar{C} turns out to be on the order of 10^6 . The insert in Figure 3 shows the adhesive stress for $\bar{C} = 10^6$. The peak stress normalized by $2W_{ad}/\delta_o$ is about 6×10^{-4} . Because the intrinsic strength, $2W_{ad}/\delta_o$, using these parameters is 10^3 MPa , the actual peak stress, *i.e.*, the adhesive strength, is $6 \times 10^{-4} \times 10^3 \text{ MPa} = 0.6 \text{ MPa}$. The elastic modulus E_M is related to C by [18]

$$E_M = \frac{\Sigma_o \sqrt{Nb}}{C} = \frac{6W_{ad}}{\delta_o} \sqrt{\frac{T}{2C}} \tag{17}$$

and its value for the given parameters is approximately 0.6 MPa . Thus, we arrive at a result showing that the adhesive strength can be reduced by thermal fluctuations of the molecules to a value on the order of the modulus for a compliant solid.

Figure 4 shows the normalized peak stress *versus* the normalized compliance for a large range of \bar{C} . Circles are obtained from numerical

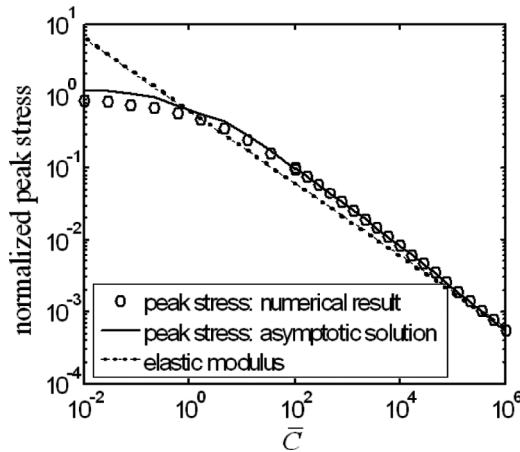


FIGURE 4 Normalized peak adhesive stress *versus* normalized compliance \bar{C} . Circles are numerical results, the solid line is an asymptotic solution, and the dashed line is the normalized elastic modulus.

integration, and the solid line is peak stress calculated using Equations (10e), (19a,b), and (20a,b) (in Section 4). On the same plot, we compare the normalized peak stress with the normalized elastic modulus, $E_M/(2W_{ad}/\delta_o)$, which is shown as the dashed line. The adhesive strength is significantly smaller than the elastic modulus for stiff materials. With increasing compliance, the adhesive strength and elastic modulus become very similar in magnitude.

The effective work of adhesion is calculated according to Equations (10c) and (10f). Figure 5 gives the numerical result (circles) for the normalized effective work of adhesion as a function of normalized compliance. It is compared with the asymptotic solution, Equations (25a,b) in section 4 (solid line). Figure 5 shows that the effective work of adhesion approaches the intrinsic work of adhesion for stiff materials ($\bar{C} \ll 1$) and decreases logarithmically with compliance for $\bar{C} \gg 1$. For $\bar{C} = 10^6$, W_{eff} is about 20% of W_{ad} . As is shown in the next section, this decrease in the effective work of adhesion is due to the difference in entropy of the bound and unbound states.

In Figures 3 and 4, we have shown by direct integration of Equations (10b) and (12) that our simple model predicts that adhesive strength can be decreased dramatically because of thermal fluctuations of molecules. This is essentially due to the fact that, by virtue of their compliance, many detached states are made available to a molecule well before the stress in the attached state reaches the maximum

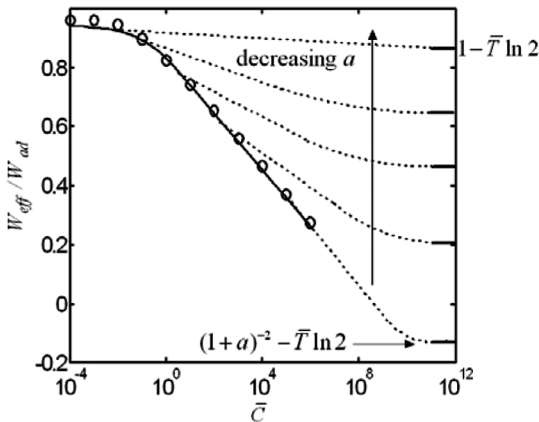


FIGURE 5 Normalized effective work of adhesion as a function of normalized compliance. Circles are numerical results. The solid line is an asymptotic solution. Dashed lines illustrate that the effective work of adhesion can be increased by modifying the linear spring model.

van der Waals stress. By the time this peak stress is reached, most chains are already in the detached state. In the next section, we analyze the model in more detail to extract its behavior in various limiting cases.

4. ASYMPTOTIC ANALYSIS

In this section, we carry out asymptotic analysis to obtain the adhesive stress and effective work of adhesion. Specifically, we give a closed-form solution for the effective work of adhesion as a function of temperature and compliance. We show that the effective work of adhesion decays logarithmically with compliance for soft materials. This decay is an entropic effect. Its magnitude can be bounded by modifying the linear spring model using a constrained potential.

The Laplace method [20] has been used for the asymptotic analysis. The basic idea is that although we explore all the possible states of the molecule, the most probable states are those in the vicinity of energy minima. Therefore, we can estimate the stress and work of adhesion by considering only contribution from those states. Specifically, because of the fast decay of the exponential function, the evaluation of the integrals $Z(\bar{u})$ in Equation (10b) and $I(\bar{u})$ in Equation (12) can be approximated by expanding the energy function about its minima. Details of the solution are given later.

4.1. Linear Spring Model

As pointed out in the previous section, we need to evaluate $Z(\bar{u})$ and $I(\bar{u})$ to obtain adhesive stress and effective work of adhesion. We focus our interest on the case of $\bar{T} \ll 1$, which corresponds to temperature lower than or of the same order as the room temperature. The Laplace method [20] tells us that, as long as $\bar{T} \ll 1$, the behavior of the integrals $Z(\bar{u})$ and $I(\bar{u})$ is determined by the behavior of the normalized energy function $\Lambda(\bar{u}, \bar{\delta})$ near its minimum. If there are two or more minima, then the integral is determined by the absolute minimum, which can occur at the boundary points. Physically this means that we can estimate the relative probabilities of state occupancy by integrating separately in the vicinity of each equilibrium state only. In this section, we use the Laplace method to obtain the asymptotic behaviors of $Z(\bar{u})$ and $I(\bar{u})$ for $\bar{T} \ll 1$ and use the results to calculate the free energy, stress, and effective work of adhesion.

We first determine the locations of the minima of $\Lambda(\bar{u}, \bar{\delta})$ for a given \bar{u} . It can be shown (see Appendix B) that the existence and locations

of the minima depend on the normalized compliance \bar{C} defined in Equation (11).

Case I: $\bar{C} \geq 1$

- 1) If $\bar{u} \leq \bar{u}_{\min} \equiv (4/3)\bar{C}^{-1/4} - 1$, then the minimum of $\Lambda(\bar{u}, \bar{\delta})$ occurs at $\bar{\delta} = 0$.
- 2) If $\bar{u}_{\min} < \bar{u} \leq \bar{u}_{\max} \equiv \bar{C}/3$, then there is one minimum at zero, maximum at $\bar{\delta}_1$ and one minimum at $\bar{\delta}_2$, and $\bar{\delta}_1 < \bar{\delta}_2$.
- 3) If $\bar{u} > \bar{u}_{\max}$, then there is only one minimum at $\bar{\delta}_2$.

Figure 6 illustrates these three situations. We have verified numerically that a good approximation to $\bar{\delta}_2$ in Cases I.2 and I.3 is

$$\bar{\delta}_2 \approx \bar{u} - \frac{0.4\bar{C}}{(1 + \bar{u})^3}. \tag{18}$$

Case II: $\bar{C} < 1$

- 1) If $\bar{u} \leq \bar{u}_{\max}$, then the minimum of $\Lambda(\bar{u}, \bar{\delta})$ occurs at $\bar{\delta} = 0$.
- 2) If $\bar{u} > \bar{u}_{\max}$, then there is only one minimum at $\bar{\delta}_2$ approximated by Equation (18).

Because of the rapid decay of the exponential factor in $Z(\bar{u})$ and $I(\bar{u})$, the simplest way of estimating these integrals is to add the two contributions from $\bar{\delta} = 0$ and $\bar{\delta} = \bar{\delta}_2$. Details of the calculation are given in Appendix C. Here we only give the final results.

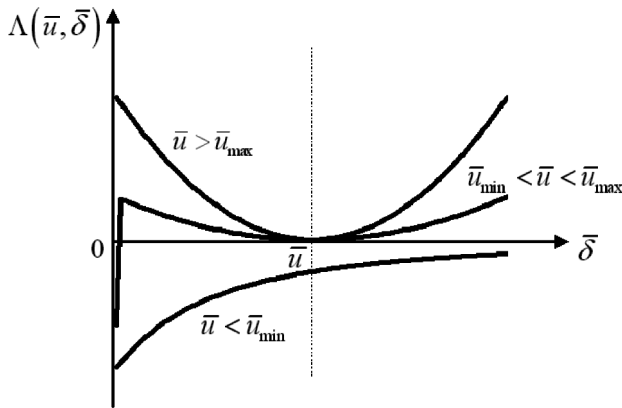


FIGURE 6 Different shapes of the normalized energy function $\Lambda(\bar{u}, \bar{\delta})$ for $\bar{u} \leq \bar{u}_{\min} \equiv 4\bar{C}^{-1/4}/3 - 1$, $\bar{u}_{\min} < \bar{u} \leq \bar{u}_{\max} \equiv \bar{C}/3$, and $\bar{u} > \bar{u}_{\max}$ in the case of $\bar{C} \geq 1$.

$\bar{C} \geq 1$:

$$Z(\bar{u}) \approx \frac{\bar{T}e^{-\Lambda(\bar{u},0)/\bar{T}}}{\Lambda'(\bar{u},0)}H(\bar{u}_{\max} - \bar{u}) + \frac{e^{-\Lambda(\bar{u},\bar{\delta}_2)/\bar{T}}}{\sqrt{2\Lambda''(\bar{u},\bar{\delta}_2)/\pi\bar{T}}}erfc\left(-\bar{\delta}_2\sqrt{\frac{\Lambda''(\bar{u},\bar{\delta}_2)}{2\bar{T}}}\right)H(\bar{u} - \bar{u}_{\min}), \quad (19a)$$

$$I(\bar{u}) \approx \frac{\bar{T}^2e^{-\Lambda(\bar{u},0)/\bar{T}}}{[\Lambda'(\bar{u},0)]^2}H(\bar{u}_{\max} - \bar{u}) + \frac{\bar{\delta}_2e^{-\Lambda(\bar{u},\bar{\delta}_2)/\bar{T}}}{\sqrt{2\Lambda''(\bar{u},\bar{\delta}_2)/\pi\bar{T}}}erfc\left(-\bar{\delta}_2\sqrt{\frac{\Lambda''(\bar{u},\bar{\delta}_2)}{2\bar{T}}}\right)H(\bar{u} - \bar{u}_{\min}). \quad (19b)$$

$\bar{C} < 1$:

$$Z(\bar{u}) \approx \frac{e^{-[\Lambda(\bar{u},0)/\bar{T} - [\Lambda'(\bar{u},0)]^2/2\bar{T}\Lambda''(\bar{u},0)]}}{\sqrt{2\Lambda''(\bar{u},0)/\pi\bar{T}}}erfc\left(\frac{\Lambda'(\bar{u},0)}{\sqrt{2\bar{T}\Lambda''(\bar{u},0)}}\right)H(\bar{u}_{\max} - \bar{u}) + \frac{e^{-\Lambda(\bar{u},\bar{\delta}_2)/\bar{T}}}{\sqrt{2\Lambda''(\bar{u},\bar{\delta}_2)/\pi\bar{T}}}erfc\left(-\bar{\delta}_2\sqrt{\frac{\Lambda''(\bar{u},\bar{\delta}_2)}{2\bar{T}}}\right)H(\bar{u} - \bar{u}_{\max}), \quad (20a)$$

$$I(\bar{u}) \approx \left[\frac{\bar{T}e^{-\Lambda(\bar{u},0)/\bar{T}}}{\Lambda'(\bar{u},0)} - \frac{\Lambda'(\bar{u},0)}{\Lambda''(\bar{u},0)} \frac{e^{-[\Lambda(\bar{u},0)/\bar{T} - [\Lambda'(\bar{u},0)]^2/2\bar{T}\Lambda''(\bar{u},0)]}}{\sqrt{2\Lambda''(\bar{u},0)/\pi\bar{T}}} \right] \times erfc\left(\frac{\Lambda'(\bar{u},0)}{\sqrt{2\bar{T}\Lambda''(\bar{u},0)}}\right)H(\bar{u}_{\max} - \bar{u}) + \frac{\bar{\delta}_2e^{-\Lambda(\bar{u},\bar{\delta}_2)/\bar{T}}}{\sqrt{2\Lambda''(\bar{u},\bar{\delta}_2)/\pi\bar{T}}}erfc\left(-\bar{\delta}_2\sqrt{\frac{\Lambda''(\bar{u},\bar{\delta}_2)}{2\bar{T}}}\right)H(\bar{u} - \bar{u}_{\max}) \quad (20b)$$

where $\Lambda'(\bar{u}, \bar{\delta})$ and $\Lambda''(\bar{u}, \bar{\delta})$ are, respectively, the first and second derivatives of $\Lambda(\bar{u}, \bar{\delta})$ with respect to $\bar{\delta}$ given by

$$\Lambda'(\bar{u}, \bar{\delta}) = -\frac{6}{\bar{C}}(\bar{u} - \bar{\delta}) + \frac{2}{(1 + \bar{\delta})^3}, \quad (21a)$$

$$\Lambda''(\bar{u}, \bar{\delta}) = \frac{6}{\bar{C}} - \frac{6}{(1 + \bar{\delta})^4}. \quad (21b)$$

In Equations (19a,b) and (20a,b), H is the Heaviside step function. It is multiplied to the second term of each equation because the local minimum $\bar{\delta}_2$ only exists if $\bar{u} > \bar{u}_{\min}$ ($\bar{C} \geq 1$) or $\bar{u} > \bar{u}_{\max}$ ($\bar{C} < 1$). A factor of $H(\bar{u}_{\max} - \bar{u})$ is multiplied to the first term in Equation (20a) because $\Lambda'(\bar{u}, 0) < 0$ for $\bar{u} > \bar{u}_{\max}$, and so that application of the Laplace method at $\bar{\delta} = 0$ is no longer valid.

The adhesive stress can be calculated using Equations (10e), (19a,b), and (20a,b). The asymptotic solution compares well with numerical result in Figure 3. The effective work of adhesion is calculated using Equations (10c,f), (19a), and (20a). According to Equation (18), as $\bar{u} \rightarrow \infty$, $\bar{\delta}_2 \rightarrow \bar{u}$. Therefore both Equations (19a) and (20a) predict

$$Z(\bar{u} \rightarrow \infty) \approx \frac{e^{-\Lambda(\bar{u}, \bar{u})/\bar{T}}}{\sqrt{2\Lambda''(\bar{u}, \bar{u})/\pi\bar{T}}} \operatorname{erfc} \left(-\bar{u} \sqrt{\frac{\Lambda''(\bar{u}, \bar{u})}{2\bar{T}}} \right) \rightarrow \sqrt{\frac{\pi\bar{C}\bar{T}}{3}}. \quad (22)$$

Equation (22) is the same as Equation (13) because the normalized energy $\Lambda(\bar{u}, \bar{\delta})$ is dominated by the harmonic potential $3(\bar{u} - \bar{\delta})/\bar{C}$ as $\bar{u} \rightarrow \infty$. Equations (A19) and (A20), the partition function as $\bar{u} \rightarrow 0$ is found to be

$$Z(\bar{u} \rightarrow 0) \approx \begin{cases} \frac{\bar{T}e^{1/\bar{T}}}{2} & \bar{C} \geq 1 \\ \frac{e^{[(1/\bar{T}) + (1/3\bar{T})(1/\bar{C} - 1)]}}{2\sqrt{3(1/\bar{C} - 1)/\pi\bar{T}}} \operatorname{erfc} \left(\frac{1}{\sqrt{3\bar{T}(1/\bar{C} - 1)}} \right) & \bar{C} < 1 \end{cases} \quad (23)$$

The normalized effective work of adhesion can now be calculated using Equations (10c) and (10f). It should be emphasized that the asymptotic behavior $Z(\bar{u} \rightarrow 0)$ given by Equation (23) is not accurate for extremely large compliance. The reason is as follows. The Laplace method works as long as the integrals are bounded. As $\bar{C} \rightarrow \infty$, the integral becomes unbounded so the method is expected to break down for large \bar{C} . Specifically, the normalized energy function, $\Lambda(0, \bar{\delta}) = 3\bar{\delta}^2/\bar{C} - 1/(1 + \bar{\delta})^2$, starts from -1 at $\bar{\delta} = 0$ and monotonically increases to infinity. For very soft materials with extremely large compliance \bar{C} , $\Lambda(0, \bar{\delta})$ is close to zero until $\bar{\delta} \cong \sqrt{\bar{C}}$. Because the asymptotic solution depends only on the local expansion of $\Lambda(0, \bar{\delta})$ about $\bar{\delta} = 0$, it ignores the large contribution from the neighborhood of $\bar{\delta} = 0$ to $\bar{\delta} \cong \sqrt{\bar{C}}$ where $\Lambda(0, \bar{\delta}) \approx 0$, i.e., $e^{-\Lambda(0, \bar{\delta})/\bar{T}} \approx 1$. Indeed, as $\bar{C} \rightarrow \infty$, $\int_0^\infty e^{-\Lambda(0, \bar{\delta})/\bar{T}} d\bar{\delta}$ is no longer governed by the

behavior of $\Lambda(0, \bar{\delta})$ at $\bar{\delta} = 0$ but rather determined by the quadratic term $3\bar{\delta}^2/\bar{C}$; that is

$$Z(\bar{u} \rightarrow 0, \bar{C} \rightarrow \infty) \approx \int_0^\infty e^{-3\bar{\delta}^2/\bar{C}\bar{T}} d\bar{\delta} = \frac{1}{2} \sqrt{\frac{\pi\bar{C}\bar{T}}{3}}. \quad (24)$$

Using Equations (10c,f), (22), (23), and (24), the normalized effective work of adhesion is found to be

$$\bar{W}_{eff} = \begin{cases} 1 + \frac{\bar{C}}{3(1-\bar{C})} + \bar{T} \left[\ln \operatorname{erfc} \left(\frac{1}{\sqrt{3\bar{T}(1/\bar{C}-1)}} \right) - \ln 2 - \frac{1}{2} \ln(1-\bar{C}) \right] & \bar{C} < 1, \\ 1 - \frac{\bar{T}}{2} \ln \frac{4\pi\bar{C}}{3\bar{T}} & \bar{C} \geq 1, \\ -\bar{T} \ln 2 & \bar{C} \rightarrow \infty. \end{cases} \quad (25a-c)$$

The solid line in Figure 5 represents the asymptotic solution (25a,b) of \bar{W}_{eff} . Figure 5 shows that \bar{W}_{eff} is underestimated by Equation (25) in the regime of $\bar{C} \ll 1$. Indeed, from Equation (25a), as $\bar{C} \rightarrow 0$, $\bar{W}_{eff} \rightarrow 1 - \bar{T} \ln 2$, which is slightly less than one because $\bar{T} \ll 1$. In the regime $\bar{C} \gg 1$, our numerical result in Figure 5 shows that \bar{W}_{eff} decays as $-\ln \bar{C}$, consistent with Equation (25b). This is because $\bar{G}(0) = -\ln Z(0)$ is independent of \bar{C} , while $\bar{G}(\infty) = -\ln Z(\infty)$ decays as $-\ln \bar{C}$. For very large \bar{C} , this decrease is purely entropic, because the mean internal energy at both bound ($\bar{u} \rightarrow 0$) and unbound ($\bar{u} \rightarrow \infty$) states are independent of \bar{C} . Specifically, the mean internal energy in the two states, calculated using Equations (10d), (22), and (23), are, respectively,

$$\langle \bar{E}(\bar{u} \rightarrow \infty) \rangle = \frac{1}{2}, \quad (26a)$$

and

$$\langle \bar{E}(\bar{u} \rightarrow 0) \rangle = \frac{1}{\bar{T}}, \quad (26b)$$

both independent of \bar{C} .

4.2. Modified Linear Spring Model

Equation (25c) indicates that for extremely compliant materials, the effective work of adhesion can be negative, which is unphysical. This unphysical result is due to the fact that the linear spring model allows

unrestricted displacements, whereas extensions of a real molecule are bounded. To explore this idea, for any \bar{u} , we constrain the motion, $\bar{\delta}$, of the springs in a box of width $2a$ centered at $\bar{u} = a$ (see Figure 7a). Within this box, the harmonic potential is maintained, whereas the potential outside the box is replaced by a rigid wall (infinite potential). For very large compliance, the harmonic potential is almost zero within the box. The total potential for $\bar{u} \rightarrow \infty$ is shown in Figure 7b. The partition function for this case is

$$Z(\bar{u} \rightarrow \infty, \bar{C} \rightarrow \infty) = \int_{\bar{u}-a}^{\bar{u}+a} (1) d\bar{\delta} = 2a. \tag{27}$$

The potential for the bounded state, $\bar{u} \rightarrow 0$, is shown in Figure 7c. The partition function for this case is

$$Z(\bar{u} \rightarrow 0, \bar{C} \rightarrow \infty) = \int_0^a e^{1/[\bar{T}(1+\bar{\delta})^2]} d\bar{\delta}. \tag{28}$$

Because $1/\bar{T}(1+a)^2 \leq 1/\bar{T}(1+\bar{\delta})^2 < 1/\bar{T}$, we find $ae^{1/\bar{T}(1+a)^2} < Z(\bar{u} \rightarrow 0, \bar{C} \rightarrow \infty) < ae^{1/\bar{T}}$. Using Equations (10c) and (10f), the effective work of adhesion must lie in the range

$$(1+a)^{-2} - \bar{T} \ln 2 < \bar{W}_{eff}(\bar{C} \rightarrow \infty) < 1 - \bar{T} \ln 2. \tag{29}$$

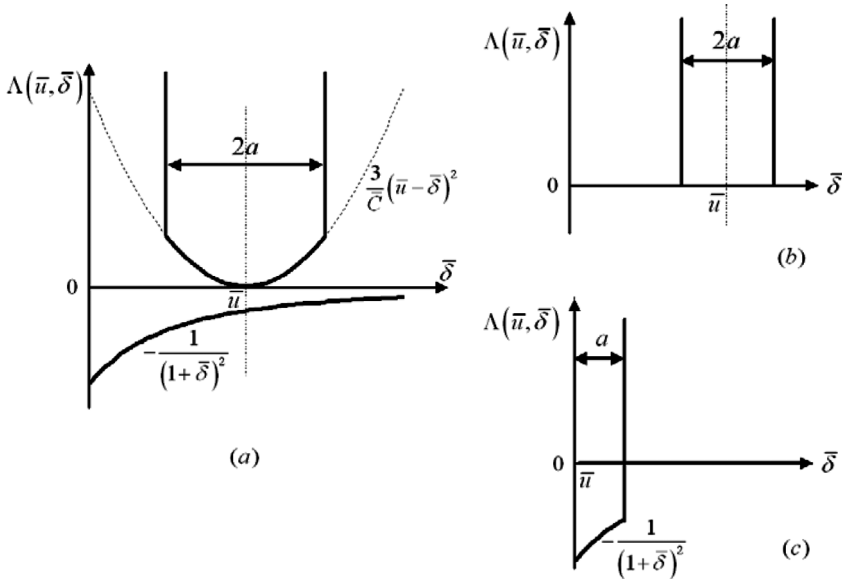


FIGURE 7 Modification of the linear spring model.

Equation (29) shows that \overline{W}_{eff} can approach different values as $\overline{C} \rightarrow \infty$ by reducing the size of the box $2a$. This effect is demonstrated by the dashed lines in Figure 5.

To conclude, the linear spring model is unrealistic at very large deformation ($u - \delta \cong Nb$). In this regime, the deformation is governed by stretching of the covalent bonds, which is represented by the infinite potential. Therefore, if we replace our linear spring model by a more realistic model of a polymer chain, the effective work of adhesion will be positive even for very large compliances. We have confirmed analytically that the introduction of a confining potential does not alter the conclusion that adhesive strength vanishes with increasing compliance. Details of this analysis are available from the authors.

5. SUMMARY AND CONCLUSIONS

We show that the adhesive stress of soft solids can be dramatically reduced by thermal fluctuation with little changes in the effective work of adhesion (change is logarithmic with compliance). The peak adhesive stress is found to be the same as the intrinsic strength for very stiff materials and is on the order of the elastic modulus for soft materials. The effective work of adhesion equals the intrinsic work of adhesion for stiff materials and decays logarithmically with compliance because of an entropic effect. For materials of practical interest, the effective work of adhesion predicted by our model is quantitatively correct. For extremely compliant solids, our model underestimates the work of adhesion. This discrepancy can be removed by using a more realistic model for chain deformation.

In this work, we have focused our interests in temperatures below or about room temperature, which is the typical situation. It is easy to see that the effective work of adhesion in the case of very high temperature is the same as the case of large compliance. First of all, the energy function is dominated by the harmonic potential in the unbound state ($\overline{u} \rightarrow \infty$). Hence, the partition function in the unbound state is still given by Equation (22). In the bound state where $\overline{u} \rightarrow 0$, the normalized energy $\Lambda(\overline{u} \rightarrow 0, \overline{\delta})$ equals $3\overline{\delta}^2/\overline{C}\overline{T} - 1/\overline{T}(1 + \overline{\delta})^2$, which is zero at high temperature (\overline{T}) except for very large $\overline{\delta}$. That is, the van der Waals potential $1/\overline{T}(1 + \overline{\delta})^2$ is negligible compared with the quadratic term $3\overline{\delta}^2/\overline{C}\overline{T}$ in the calculation of the partition function in the bound state. This is the same situation as the case of large compliance (\overline{C}). In addition, the normalized compliance, \overline{C} , and temperature, \overline{T} , play the same role in the dominant term $3\overline{\delta}^2/\overline{C}\overline{T}$ of the energy and thus in the evaluation of the partition function. According

to Equations (10c,f), the effective work of adhesion is, therefore, the same for high temperature and large compliance.

In our model, the molecules bridging the interface are under thermodynamic equilibrium. Irreversible processes such as breaking of covalent bonds have not been considered. As pointed out by Lake and Thomas [21], the work of fracture can be greatly amplified because of the stretching of the covalent bonds in the molecule, because all the energy stored in the bonds is lost upon breaking of one bond. This effect is not included in our model.

We also have not considered in our model any rate effect, viscoelasticity, or nonlinearity that may significantly increase the adhesive strength and effective work of adhesion. For example, it has been observed that for polymer gels or pressure-sensitive adhesives, the decohesion strength remains in the MPa range whereas the modulus can drop to the kPa range. One possible explanation is that the materials on the interface can be locally stiffened; *i.e.*, the local modulus can be much higher than the bulk modulus. The nonlinearity can be included by modifying the spring model, but it will make the result much harder to interpret and is out of the scope of this work.

Lastly, our model can be applied to the case of a crack, where there is a displacement profile behind the crack tip. The relation obtained in this work between the adhesive stress, σ , and the separation, u , can be used for a generic point on the crack face. In this case, our model would serve as a cohesive zone model. The focus of our work has been on the strength of a layer of adhesive molecules that, for compliant materials, can reasonably be expected to be in thermodynamic equilibrium. Because the molecules that make up the adhesive region are the same as those in the bulk, their properties allow us to relate adhesive strength to bulk compliance. However, we do not specifically consider the mechanics and thermodynamics of the exterior body itself.

ACKNOWLEDGMENTS

This work was supported in part by the National Science Foundation, grant CMS-0527785.

APPENDIX A

The total energy consists of two contributions. The first is the entropic loss of the molecules when they leave the bulk. Assuming the molecules bridging the two interfaces are linear entropic springs with compliance, C , the energy of each spring due to its stretch is

$$E_e(u, \delta) = \frac{(u - \delta)^2}{2C}, \quad (\text{A1})$$

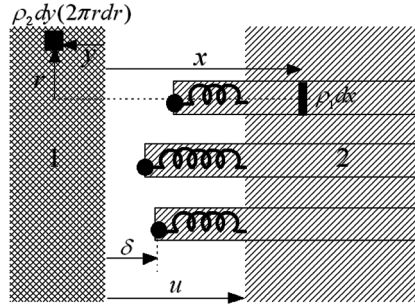


FIGURE A1 Calculating the van der Waals energy associated with a particular molecule by the interaction between a half space (solid 1 on the left) and a column (on the right), which starts from the open end of the molecule and extends to infinity.

where u and δ are shown in Figure 1. The other contribution is the adhesive interaction between the two surfaces. That associated with a particular molecule can be calculated by the van der Waals energy between a half space and a column starting from the open end of the molecule extending to infinity, as shown in Figure A1.

Using a 6–12 Lennard–Jones potential for two atoms at a distance of R ,

$$V(R) = -\frac{A}{R^6} + \frac{B}{R^{12}}, \tag{A2}$$

the van der Waals energy between the half space and a column of unit area is

$$\begin{aligned} w(\delta) &= \int_{\delta}^{\infty} \int_0^{\infty} \int_0^{\infty} (\rho_2 dx)(\rho_1 2\pi r dr dy) \\ &\quad \times \left[-\frac{A}{(\sqrt{(x+y)^2 + r^2})^6} + \frac{B}{(\sqrt{(x+y)^2 + r^2})^{12}} \right] \\ &= 2\pi\rho_2\rho_1 \left(-\frac{A}{24\delta^2} + \frac{B}{720\delta^8} \right), \end{aligned} \tag{A3}$$

where ρ_1 is the number of atoms per unit length in the half space, and ρ_2 is the number of atoms per unit length in the column. Note that Equation (A3) has an attractive part and a repulsive part. For simplicity, we replace the repulsive part with a hard wall. To do this, we first find the equilibrium distance, δ_o , by differentiating Equation (A3) with respect to δ and setting the result equal to zero. This results in

$$\delta_o = \left(\frac{2B}{15A} \right)^{1/6}. \tag{A4}$$

By maintaining $w(\delta)$ in Equation (A3) for $\delta \geq \delta_o$ while replacing $w(\delta < \delta_o)$ with a hard wall, we can write the van der Waals energy as

$$w(\delta) = -\frac{W_{ad}}{\Sigma_o} \left(\frac{\delta_o}{\delta + \delta_o} \right)^2, \quad (\text{A5})$$

where

$$\frac{W_{ad}}{\Sigma_o} \equiv \frac{\pi\rho_1\rho_2A}{12\delta_o^2}. \quad (\text{A6})$$

Σ_o in Equation (A6) is the number of molecules per unit area on the surface, and W_{ad} can be identified as the intrinsic work of adhesion. Note that the coordinate δ in Equation (A5) has been shifted by δ_o so that the range of δ is from 0 to infinity. At $\delta = 0$ (in contact), Equation (A5) reduces to $w(0) = -W_{ad}/\Sigma_o$, as expected.

The total energy, E , associated with a particular molecule is the sum of Equations (A1) and (A5), which results in Equation (1).

APPENDIX B

Here we look for the stationary points of the function $\Lambda(\bar{u}, \bar{\delta})$. Differentiating $\Lambda(\bar{u}, \bar{\delta})$ with respect to $\bar{\delta}$ and setting it equal to zero give

$$\frac{3}{C}(\bar{u} - \bar{\delta}) = \frac{1}{(1 + \bar{\delta})^3}. \quad (\text{A7})$$

This can be rewritten as

$$X + \frac{1}{X^3} = Y \quad (\text{A8})$$

by defining

$$X \equiv \frac{1 + \bar{\delta}}{(C/3)^{1/4}}, \quad (\text{A9})$$

$$Y \equiv \frac{1 + \bar{u}}{(C/3)^{1/4}}. \quad (\text{A10})$$

It can be easily verified (illustrated by Figure A2) that Equations (A8) has no solution (*i.e.*, $\Lambda(\bar{u}, \bar{\delta})$ has no interior stationary points) if

$$Y < Y_{\min} \equiv \frac{4}{3^{3/4}}. \quad (\text{A11})$$

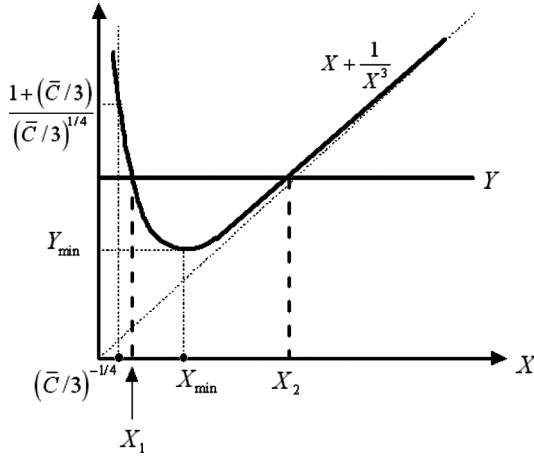


FIGURE A2 Graph of $d\Lambda(\bar{u}, \bar{\delta})/d\bar{\delta} = 0$.

Thus, $\Lambda(\bar{u}, \bar{\delta})$ is monotonically increasing as long as

$$\bar{u} < \bar{u}_{\min} \equiv \frac{4}{3}\bar{C}^{-1/4} - 1. \tag{A12}$$

For $Y > Y_{\min}$, there are two stationary points. Denote these points by $X_1(\bar{u})$ and $X_2(\bar{u})$ respectively. They satisfy $X_1(\bar{u}) < 3^{1/4} \equiv X_{\min} < X_2(\bar{u})$. The stationary point that lies to the right of X_{\min} is a local minimum, whereas the stationary point that lies to the left of X_{\min} is a local maximum. These facts can be verified by noting that

$$\Lambda''(\bar{u}, \bar{\delta} < \bar{\delta}_{\min}) < \Lambda''(\bar{u}, \bar{\delta} = \bar{\delta}_{\min}) = 0 < \Lambda''(\bar{u}, \bar{\delta} > \bar{\delta}_{\min}) \tag{A13}$$

where

$$\bar{\delta}_{\min} \equiv X_{\min}(\bar{C}/3)^{1/4} - 1. \tag{A14}$$

However, the local maximum exists only when $\bar{\delta} > 0$. According to Equation (A9), this requires

$$X_1(\bar{u}) > \frac{1}{(\bar{C}/3)^{1/4}}, \tag{A15}$$

which in turn, implies that

$$Y < \frac{1}{(\bar{C}/3)^{1/4}} + \left(\frac{\bar{C}}{3}\right)^{3/4} = \frac{1 + (\bar{C}/3)}{(\bar{C}/3)^{1/4}}. \tag{A16}$$

Note that because $\bar{u} = Y(\bar{C}/3)^{1/4} - 1$, the corresponding normalized displacement is $\bar{C}/3$. This is the reason why for $\bar{u} > \bar{u}_{\max} \equiv \bar{C}/3$, there is only one stationary point, *i.e.*, $X_2(\bar{u})$. Also, we have verified numerically that for $\bar{u} > \bar{u}_{\min}$, a good approximation to the local minimum is

$$X_2 \approx Y - \frac{1.2}{Y^3}. \quad (\text{A17})$$

It should be noted that this above analysis implicitly assumes that $(\bar{C}/3)^{-1/4} < 3^{1/4}$ (see Figure A2). However, if $\bar{C} < 1$, then $(\bar{C}/3)^{-1/4} > 3^{1/4}$. In this case, Equation (A8) has no solutions for $\bar{\delta} > 0$ unless $\bar{u} > \bar{u}_{\max}$. For $\bar{u} > \bar{u}_{\max}$, the only solution to Equation (A8) is a local minimum and is given also by Equation (18).

APPENDIX C

We calculate the contribution to $Z(\bar{u})$ and $I(\bar{u})$ from the minima of the normalized energy function $\Lambda(\bar{u}, \bar{\delta})$. As noted in Appendix B, the minimum of $\Lambda(\bar{u}, \bar{\delta})$ either occurs at $\bar{\delta} = 0$ or at $\bar{\delta}_2 \approx \bar{u} - 0.4\bar{C}/(1 + \bar{u})^3$. The local expansion of $\Lambda(\bar{u}, \bar{\delta})$ about $\bar{\delta} = 0$ is

$$\Lambda(\bar{u}, \bar{\delta}) = \Lambda(\bar{u}, 0) + \Lambda'(\bar{u}, 0)\bar{\delta} + \frac{\Lambda''(\bar{u}, 0)}{2}\bar{\delta}^2 + \dots, \quad (\text{A18})$$

where $\Lambda'(\bar{u}, \bar{\delta})$ and $\Lambda''(\bar{u}, \bar{\delta})$ indicate the first and second derivatives of $\Lambda(\bar{u}, \bar{\delta})$ with respect to $\bar{\delta}$. To keep the linear term of Equation (A18) in the evaluation of $Z(\bar{u})$ and $I(\bar{u})$, we must insist that $\Lambda'(\bar{u}, 0) > 0$, which requires $\bar{u} < \bar{u}_{\max} \equiv \bar{C}/3$. Similarly, in order to keep the quadratic term, $\Lambda''(\bar{u}, 0) > 0$, which requires $\bar{C} < 1$. Therefore, for $\bar{C} \geq 1$, $Z(\bar{u})$ and $I(\bar{u})$ near $\bar{\delta} = 0$ are determined by keeping the linear terms of $\Lambda(\bar{u}, \bar{\delta})$ about $\bar{\delta} = 0$:

$$Z(\bar{u}) \approx \int_0^\infty e^{-[\Lambda(\bar{u}, 0) + \Lambda'(\bar{u}, 0)\bar{\delta}]/\bar{T}} d\bar{\delta} = \frac{\bar{T} e^{-\Lambda(\bar{u}, 0)/\bar{T}}}{\Lambda'(\bar{u}, 0)}, \quad (\text{A19})$$

$$I(\bar{u}) \approx \int_0^\infty \bar{\delta} e^{-[\Lambda(\bar{u}, 0) + \Lambda'(\bar{u}, 0)\bar{\delta}]/\bar{T}} d\bar{\delta} = \frac{\bar{T}^2 e^{-\Lambda(\bar{u}, 0)/\bar{T}}}{[\Lambda'(\bar{u}, 0)]^2}. \quad (\text{A20})$$

For $\bar{C} < 1$, $Z(\bar{u})$, and $I(\bar{u})$ near $\bar{\delta} = 0$ are determined by keeping the linear and quadratic terms of $\Lambda(\bar{u}, \bar{\delta})$ about $\bar{\delta} = 0$:

$$\begin{aligned} Z(\bar{u}) &\approx \int_0^\infty e^{-[\Lambda(\bar{u}, 0) + \Lambda'(\bar{u}, 0)\bar{\delta} + \Lambda''(\bar{u}, 0)\bar{\delta}^2/2]/\bar{T}} d\bar{\delta} \\ &= \frac{e^{-[\Lambda(\bar{u}, 0)/\bar{T} - [\Lambda'(\bar{u}, 0)]^2/2\bar{T}\Lambda''(\bar{u}, 0)]}}{\sqrt{2\Lambda''(\bar{u}, 0)/\pi\bar{T}}} \operatorname{erfc} \left(\frac{\Lambda'(\bar{u}, 0)}{\sqrt{2\bar{T}\Lambda''(\bar{u}, 0)}} \right), \end{aligned} \quad (\text{A21})$$

$$\begin{aligned}
I(\bar{u}) &\approx \int_0^\infty \bar{\delta} e^{-[\Lambda(\bar{u},0) + \Lambda'(\bar{u},0)\bar{\delta} + \Lambda''(\bar{u},0)\bar{\delta}^2/2]/\bar{T}} d\bar{\delta} \\
&= \frac{\bar{T} e^{-\Lambda(\bar{u},0)/\bar{T}}}{\Lambda''(\bar{u},0)} - \frac{\Lambda'(\bar{u},0)}{\Lambda''(\bar{u},0)} \frac{e^{-[\Lambda(\bar{u},0)/\bar{T} - [\Lambda'(\bar{u},0)]^2/2\bar{T}\Lambda''(\bar{u},0)]}}{\sqrt{2\Lambda''(\bar{u},0)/\pi\bar{T}}} \\
&\quad \times \operatorname{erfc} \left(\frac{\Lambda'(\bar{u},0)}{\sqrt{2\bar{T}\Lambda''(\bar{u},0)}} \right) \tag{A22}
\end{aligned}$$

It can be shown (using the asymptotic behavior of the complementary error function) that Equations (A21) and (A22) agree with Equations (A19) and (A20) as $\bar{C} \rightarrow 1$. Following the same approach, $Z(\bar{u})$ and $I(\bar{u})$ near the local minimum $\bar{\delta}_2$, if it exists, are found to be

$$Z(\bar{u}) \approx \frac{e^{-\Lambda(\bar{u},\bar{\delta}_2)/\bar{T}}}{\sqrt{2\Lambda''(\bar{u},\bar{\delta}_2)/\pi\bar{T}}} \operatorname{erfc} \left(-\bar{\delta}_2 \sqrt{\frac{\Lambda''(\bar{u},\bar{\delta}_2)}{2\bar{T}}} \right), \tag{A23}$$

$$I(\bar{u}) \approx \frac{\bar{\delta}_2 e^{-\Lambda(\bar{u},\bar{\delta}_2)/\bar{T}}}{\sqrt{2\Lambda'(\bar{u},\bar{\delta}_2)/\pi\bar{T}}} \operatorname{erfc} \left(-\bar{\delta}_2 \sqrt{\frac{\Lambda''(\bar{u},\bar{\delta}_2)}{2\bar{T}}} \right), \tag{A24}$$

where $\Lambda''(\bar{u},\bar{\delta}_2)$ can be shown to be positive using the approximation (18) and $\bar{u} > \bar{u}_{\min} \equiv (4/3)\bar{C}^{1/4} - 1$, which is the condition for $\bar{\delta}_2$ to exist. The simplest way of estimating $Z(\bar{u})$ and $I(\bar{u})$ is to add the two contributions together, resulting in Equations (19a,b) and (20a,b).

REFERENCES

- [1] Israelachvili, J. N., *Intermolecular and Surface Forces* (Academic Press, London, 1991), 2nd ed.
- [2] Dugdale, D. S., *J. Mech. Phys. Solids* **8**, 100–104 (1960).
- [3] Barenblatt, G. I., *Adv. Appl. Mech.* **7**, 55–129 (1962).
- [4] Hui, C. Y., Jagota, A., Bennison, S. J., and Londono, J. D., *Proc. Roy. Soc. London A* **459**, 1489–1516 (2003).
- [5] Gent, A. N. and Wang, C., *J. Mater. Sci.* **26**, 3392–3395 (1991).
- [6] Tvergaard, V. and Hutchinson, J. W., *J. Mech. Phys. Solids* **40**, 1377–1397 (1992).
- [7] Schapery, R. A., *Int. J. Fracture* **39**, 163–189 (1989).
- [8] Mazur, S. and Plazek, D. J., *Prog. Org. Coat.* **24**, 225–236 (1994).
- [9] Lin, Y. Y., Hui, C. Y., and Jagota, A., *J. Colloid Interface. Sci.* **237**, 267–282 (2001).
- [10] Jagota, A., Bennison, S. J., and Smith, C. A., *Int. J. Fracture* **104**, 105–130 (2000).
- [11] Ghatak, A., Mahadevan, L., Chung, J. Y., Chaudhury, M. K., and Shenoy, V., *Proc. Roy. Soc. London A* **460**, 2725–2735 (2004).
- [12] Chung, J. Y. and Chaudhury, M. K., *J. Roy. Soc. Interface* **2**, 55–61 (2005).

- [13] Johnson, K. L., Kendall, K., and Roberts, A. D., *Proc. Roy. Soc. London A* **324**, 301–313 (1971).
- [14] Chaudhury, M. K. and Whitesides, G. M., *Langmuir* **7**, 1013–1025 (1991).
- [15] Chaudhury, M. K., *J. Phys. Chem. B* **103**, 6562–6566 (1999).
- [16] Ghatak, A., Vorvolakos, K., She, H., Malotky, D. L., and Chaudhury, M. K., *J. Phys. Chem. B* **104**, 4018–4030 (2000).
- [17] Hui, C. Y., Tang, T., Lin, Y. Y., and Chaudhury, M. K., *Langmuir* **20**, 6052–6064 (2004).
- [18] Rubinstein, M. and Colby, R. H., *Polymer Physics* (Oxford University Press, New York, 2003).
- [19] Hill, T. L., *An Introduction to Statistical Thermodynamics* (Dover, New York, 1986).
- [20] Carrier, G. F., Krook, M., and Pearson, C. E., *Functions of Complex Variables* (McGraw Hill, New York, 1966).
- [21] Lake, G. J. and Thomas, A. G., *Proc. R. Soc. London, A* **300**, 108–119 (1967).